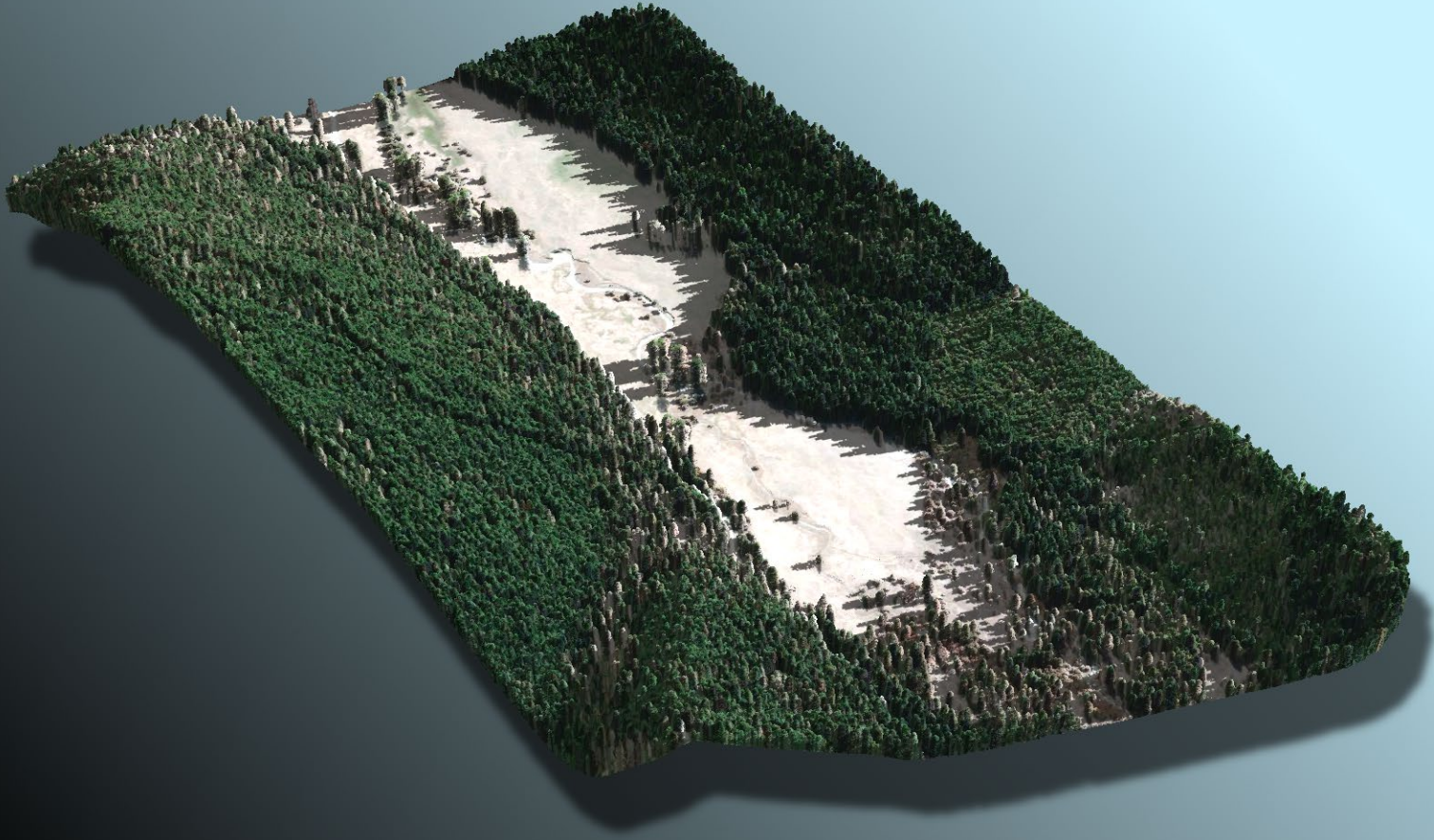


July 9, 2019



Mineral County Tributaries, Montana LiDAR

Technical Data Report

Prepared For:

Michael Baker

I N T E R N A T I O N A L

Kevin Doyle

Michael Baker International
165 S. Union Blvd., Suite 1000
Lakewood, CO 80228
PH: 720-514-1100

Prepared By:



QSI Corvallis

1100 NE Circle Blvd, Ste. 126
Corvallis, OR 97330
PH: 541-752-1204

TABLE OF CONTENTS

INTRODUCTION	1
Deliverable Products	2
ACQUISITION	4
Planning.....	4
Airborne LiDAR Survey	6
Ground Survey.....	8
Monumentation	8
Ground Survey Points (GSPs).....	9
PROCESSING	11
LiDAR Data.....	11
Feature Extraction	Error! Bookmark not defined.
Contours	14
RESULTS & DISCUSSION.....	15
LiDAR Density	15
LiDAR Accuracy Assessments	21
LiDAR Non-Vegetated Vertical Accuracy	21
LiDAR Relative Vertical Accuracy	24
LiDAR Horizontal Accuracy	25
CERTIFICATIONS	26
SELECTED IMAGE	27
GLOSSARY	28
APPENDIX A - ACCURACY CONTROLS	29

Cover Photo: A view looking south at Tamarack Creek within the northernmost AOI of the 2019 LiDAR acquisition. The image was created from the LiDAR bare earth model colored by elevation and overlaid with Virtual Earth Satellite imagery and the above ground point cloud.

INTRODUCTION

This photo taken by QSI acquisition staff shows a view of GNSS equipment set up over monument MIN_CO_TRIB_01, centrally located to the 2019 sites of LiDAR acquisition in St. Regis, Montana.



In February 2019, Quantum Spatial (QSI) was contracted by the State of Montana’s Department of Natural Resources and Conservation (MTDNRC) to collect Light Detection and Ranging (LiDAR) data in the spring of 2019 for the Mineral County Tributaries site in Montana. This data acquisition serves as an 829 acre expansion to data previously provided to MTDNRC in July and November of 2017, corresponding to the Clark Fork and St. Regis project sites, respectively. Two additional adjoining areas to the 2017 St. Regis project site, comprised of data from the 2017 St. Regis acquisition, have also been processed and provided to MTDNRC as part of the Mineral County Tributaries contract. In addition, the Mineral County Tributaries project site includes topobathymetric data originally acquired in the fall of 2016, adjoining the 2017 Clark Fork project site. Reprocessed areas of interest utilized from St. Regis and Clark Fork acquisitions represent areas outside the original survey boundary extents. Data were collected to aid MTDNRC in assessing the topographic and geophysical properties of the study area in support of natural resources management and flood hazard assessment in Mineral County.

This report accompanies the delivered LiDAR data and documents contract specifications, data acquisition procedures, processing methods, and analysis of the final dataset including LiDAR accuracy and density. Acquisition dates and acreage are shown in Table 1, a complete list of contracted deliverables provided to MTDNRC is shown in Table 2, and the project extent is shown in Figure 1.

Table 1: Acquisition dates, acreage, and data types collected on the Mineral County Tributaries site

Project Site(s)	Contracted Acres	Buffered Acres	Acquisition Dates	Data Type
Clark Fork, St. Regis Add-on	568	829	4/25/2019	NIR LiDAR
Clark Fork Reprocessed	687	992	11/20/2016, 11/24/2016	Green LiDAR
St. Regis Reprocessed	113	227	8/1/2017, 8/22/2017	NIR LiDAR

Deliverable Products

Table 2: Products delivered to MTDNRC for the Mineral County Tributaries site

Mineral County Tributary LiDAR Products Projection: Montana State Plane FIPS 2500 Horizontal Datum: NAD83 (2011) Vertical Datum: NAVD88 (GEOID12A- Reprocessed AOIs, GEOID12B- Addon AOIs) Horizontal Units: International Feet Vertical Units: US Survey Feet	
Points	LAS v 1.2 <ul style="list-style-type: none"> • Raw Calibrated Swaths • All Classified Returns
Rasters	Bare Earth Digital Elevation Models (DEM) <ul style="list-style-type: none"> • 3.0 Foot Pixel Resolution • GeoTIFF Format • ESRI File Geodatabase Raster Dataset Format (*.gdb) • Space Delimited ASCII Files (*.asc) • Bathymetric Void Clipped DEM Pertaining to Clark Fork AOI Ground Density Raster Model: <ul style="list-style-type: none"> • 3.0 Foot Pixel Resolution • GeoTIFF Format
Vectors	Shapefiles (*.shp): <ul style="list-style-type: none"> • Site Boundary • Tile Index • Ground Survey Data • Total Area Flown • 1.0 Foot Contours ESRI Geodatabase (*.gdb) <ul style="list-style-type: none"> • 1.0 Foot Contours • 2D Water’s Edge Breaklines

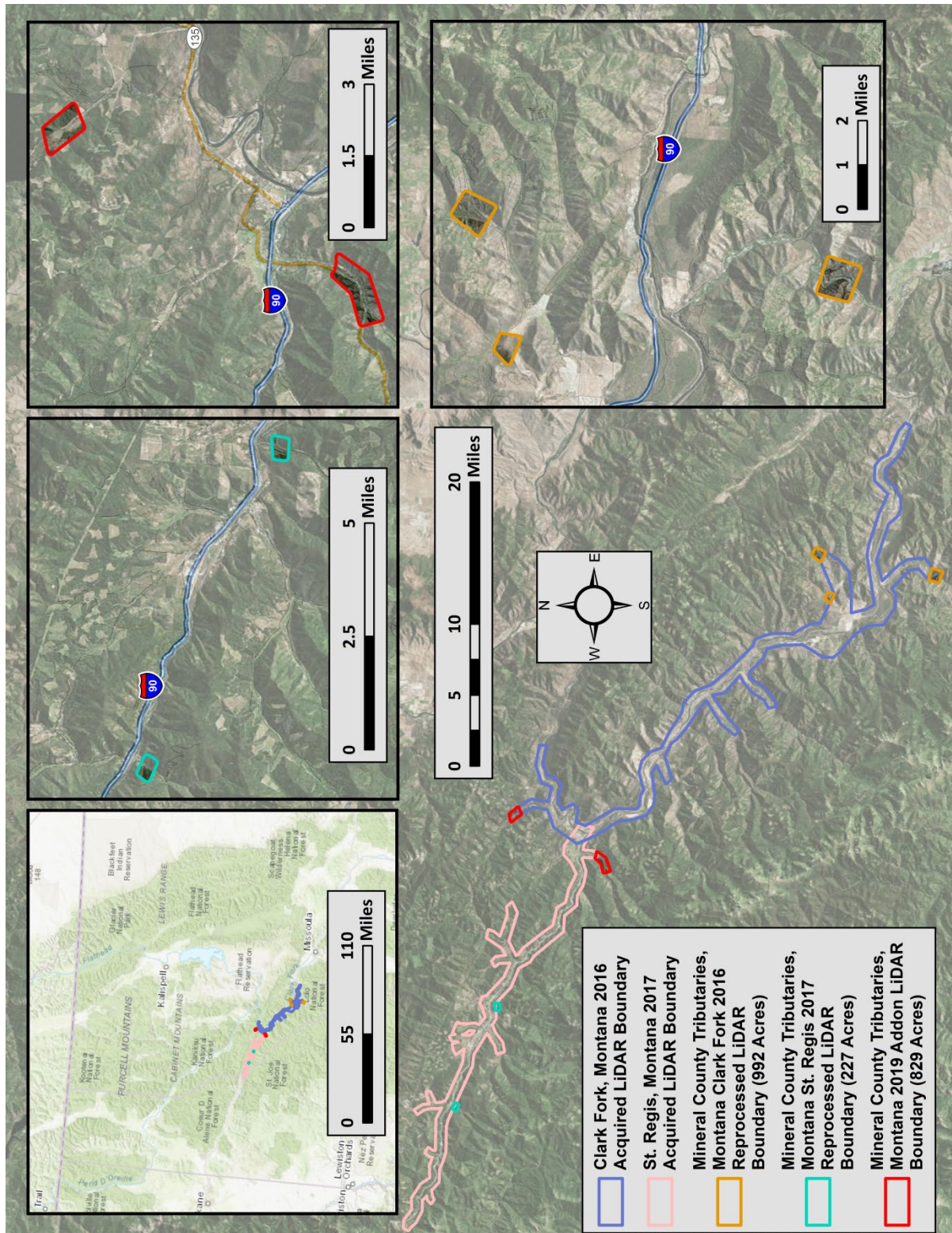


Figure 1: Location map of the Mineral County Tributaries site in Montana

QSI's Cessna Caravan



Planning

In preparation for data collection, QSI reviewed the project area and developed a specialized flight plan to ensure complete coverage of the Mineral County Tributaries LiDAR study area at the target point density of ≥ 8.0 points/m² (0.74 points/ft²). Acquisition parameters including orientation relative to terrain, flight altitude, pulse rate, scan angle, and ground speed were adapted to optimize flight paths and flight times while meeting all contract specifications.

Factors such as satellite constellation availability and weather windows must be considered during the planning stage. Any weather hazards or conditions affecting the flight were continuously monitored due to their potential impact on the daily success of airborne and ground operations. In addition, logistical considerations including private property access and potential air space restrictions were reviewed. The flight plans utilized in acquisition of the 2019 add-on data in addition to the reprocessed areas pertaining to the 2016 and 2017 LiDAR acquisitions can be visualized in Figure 2.

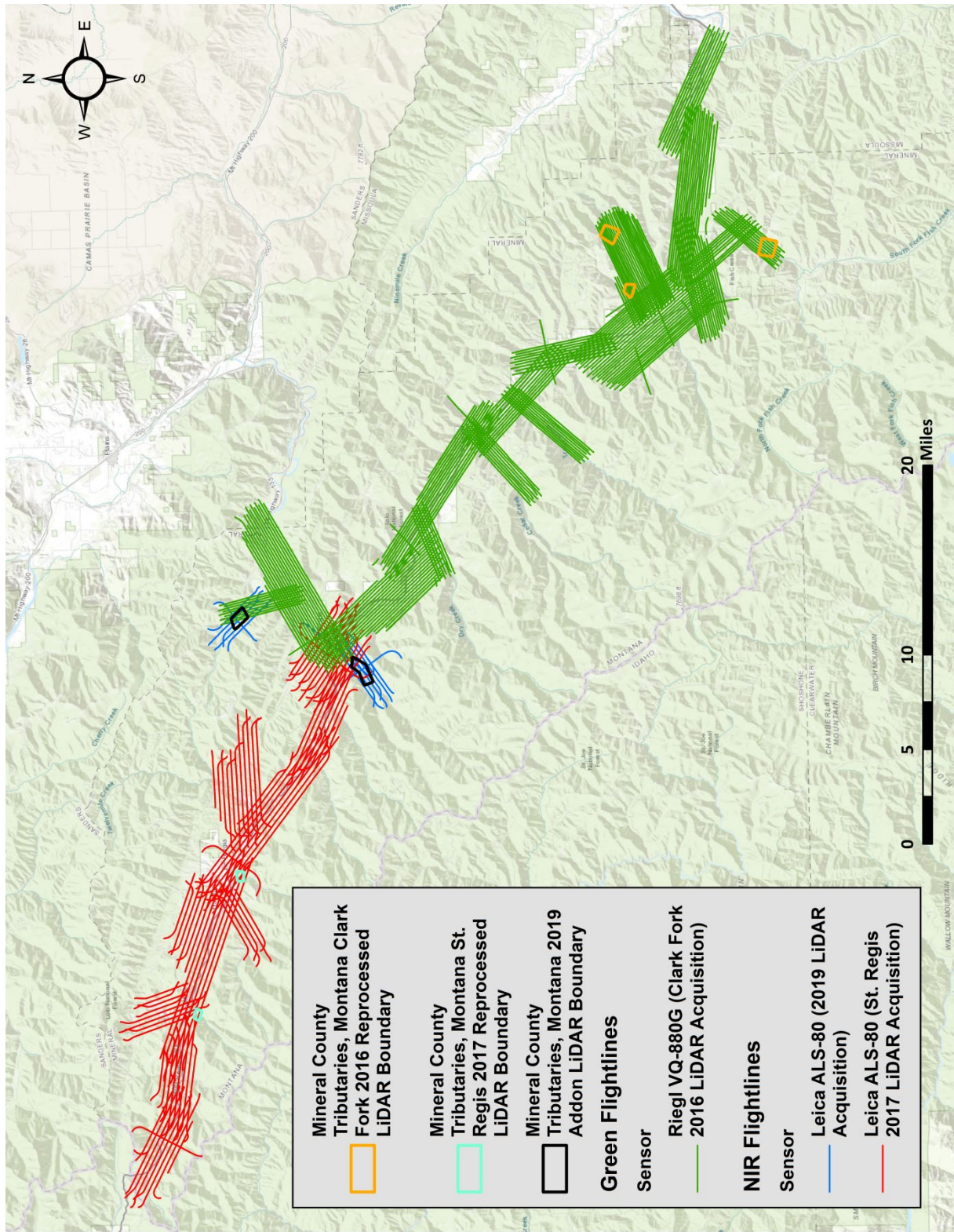


Figure 2: Mineral County Tributaries Flightline Map

Airborne LiDAR Survey

The 2019 LiDAR survey was accomplished using a Leica ALS80-HP system mounted in a Cessna Caravan. The 2016 Clark Fork and 2017 St. Regis LiDAR surveys pertaining to reprocessed areas, respectively utilized Riegl VQ-880 and Leica ALS80 systems. Table 3 summarizes the settings used to yield an average pulse density of ≥ 8 pulses/m² over the Mineral County Tributaries project area. The Riegl VQ-880-G uses a green wavelength ($\lambda=532$ nm) laser that is capable of collecting high resolution vegetation and topography data, as well as penetrating the water surface with minimal spectral absorption by water. The Leica ALS80 and VQ-880-G laser systems can record unlimited range measurements (returns) per pulse. It is not uncommon for some types of surfaces (e.g., dense vegetation or water) to return fewer pulses to the LiDAR sensor than the laser originally emitted. The discrepancy between first return and overall delivered density will vary depending on terrain, land cover, and the prevalence of water bodies. All discernible laser returns were processed for the output dataset.

Table 3: LiDAR specifications and survey settings

LiDAR Survey Settings & Specifications			
Survey	Mineral County Tributaries	Clark Fork, Mineral County	St. Regis River, Beaverhead County
Acquisition Dates	4/25/2019	11/20/2016, 11/24/2016	8/1/2017, 8/22/2017
Aircraft Used	Cessna Caravan	Cessna Caravan	Cessna Caravan
Sensor	Leica	Riegl	Leica
Laser	ALS80-HP	VQ-880-G	ALS80
Maximum Returns	Unlimited	Unlimited	Unlimited
Resolution/Density	Average 8 pulses/m ²	Average 4 pulses/m ²	Average 8 pulses/m ²
Nominal Pulse Spacing	0.35 m	0.5 m	0.35 m
Survey Altitude (AGL)	1,900 m	1,030 m	1,600 m
Survey speed	110 knots	100 knots	110 knots
Field of View	30°	40°	40°
Mirror Scan Rate	54.5 Hz	53.8 Hz	50-52 Hz
Target Pulse Rate	295 kHz	245 kHz	320 – 340 kHz
Pulse Length	2.5 ns	1.3 ns	2.5 ns
Laser Pulse Footprint Diameter	41.8 cm	1.03 m	35.2 cm
Central Wavelength	1,064 nm	532 nm	1,064 nm
Pulse Mode	Multi- Pulse in Air (MPiA)	Multi-Pulse in Air (MPiA)	Multi-Pulse in Air (MPiA)
Beam Divergence	0.22 mrad	0.7 mrad	0.22 mrad
Swath Width	1,018 m	750 m	1,165 m
Swath Overlap	54%	60%	67%
Intensity	8-bit, scaled to 16-bit	16-bit	8 bit, scaled to 16-bit
Accuracy	RMSE _z (Non-Vegetated) \leq 20 cm at 95% confidence interval	RMSE _z (Non-Vegetated) \leq 30 cm 95% confidence interval	RMSE _z (Non-Vegetated) \leq 10 cm 95% confidence interval
	Horizontal Accuracy (σ) \leq 30 cm	Horizontal Accuracy (σ) \leq 50 cm	Horizontal Accuracy (σ) \leq 30 cm

All areas were surveyed with an opposing flight line side-lap of $\geq 50\%$ ($\geq 100\%$ overlap) in order to reduce laser shadowing and increase surface laser painting. To accurately solve for laser point position (geographic coordinates x, y and z), the positional coordinates of the airborne sensor and the attitude of the aircraft were recorded continuously throughout the LiDAR data collection mission. Position of the aircraft was measured twice per second (2 Hz) by an onboard differential GPS unit, and aircraft attitude was measured 200 times per second (200 Hz) as pitch, roll and yaw (heading) from an onboard inertial measurement unit (IMU). To allow for post-processing correction and calibration, aircraft and sensor position and attitude data are indexed by GPS time. QSI utilized TerraPos Precise Point Positioning (PPP) processing techniques to post-process the LiDAR flight trajectories with a high level of position accuracy without the use of a static base station.

Ground Survey

Ground control surveys, including monumentation and ground survey point (GSP) collection, were conducted to support the airborne acquisition. Ground control data were used to geospatially correct the aircraft positional coordinate data and to perform quality assurance checks on final LiDAR data.

Monumentation

Ground survey monument MIN_CO_TRIB_01 was utilized for collection of ground survey points using post processed kinematic (PPK) survey techniques for the 2019 LiDAR acquisition. Please see the St. Regis River and Clark Fork reports for a discussion of monumentation and survey methodology utilized for the 2016 and 2017 surveys pertaining to the reprocessed areas of the Mineral County Tributaries project site.

QSI established one new monument for the Mineral County Tributaries LiDAR project (Table 4, Figure 3). The monument location was selected with consideration for satellite visibility, field crew safety, and optimal location for GSP coverage. New monumentation was set using 5/8" x 30" rebar topped with stamped 2 ½ " aluminum caps. QSI's professional land surveyor, Steven J. Hyde (MTPLS#60192 LS) oversaw and certified the monuments' establishment.

Table 4: Monument positions for the Mineral County Tributaries acquisition.
Coordinates are on the NAD83 (2011) datum, epoch 2010.00

Monument ID	Latitude	Longitude	Ellipsoid (meters)
MIN_CO_TRIB_01	47° 18' 02.08477"	-115° 05' 36.63542"	785.1395

QSI utilized static Global Navigation Satellite System (GNSS) data collected at 1 Hz recording frequency for the survey monument. During post-processing, the static GNSS data were triangulated with nearby Continuously Operating Reference Stations (CORS) using the Online Positioning User Service (OPUS¹) for precise positioning. Multiple independent sessions over the same monument were processed to confirm antenna height measurements and to refine position accuracy.

Monuments were established according to the national standard for geodetic control networks, as specified in the Federal Geographic Data Committee (FGDC) Geospatial Positioning Accuracy Standards for geodetic networks.² This standard provides guidelines for classification of monument quality at the 95% confidence interval as a basis for comparing the quality of one control network to another. The monument rating for this project is shown in Table 5.

¹ OPUS is a free service provided by the National Geodetic Survey to process corrected monument positions. <http://www.ngs.noaa.gov/OPUS>.

² Federal Geographic Data Committee, Geospatial Positioning Accuracy Standards (FGDC-STD-007.2-1998). Part 2: Standards for Geodetic Networks, Table 2.1, page 2-3. <http://www.fgdc.gov/standards/projects/FGDC-standards-projects/accuracy/part2/chapter2>

Table 5: Federal Geographic Data Committee monument rating for network accuracy

Direction	Rating
1.96 * St Dev _{NE} :	0.020 m
1.96 * St Dev _z :	0.020 m

For the Mineral County Tributaries LiDAR project, the monument coordinates contributed no more than 2.8 cm of positional error to the geolocation of the final ground survey points and LiDAR, with 95% confidence.

Ground Survey Points (GSPs)

Ground survey points were collected using post-processed kinematic (PPK) survey techniques. PPK surveys compute corrections to raw GNSS logs obtained by the rover and base station during post-processing to achieve a high level of accuracy. PPK surveys record data while stationary for at least five seconds, calculating the position using at least three one-second epochs. All GSP measurements were made during periods with a Position Dilution of Precision (PDOP) of ≤ 3.0 with at least six satellites in view of the stationary and roving receivers. See Table 6 for Trimble unit specifications.

GSPs were collected in areas where good satellite visibility was achieved on paved roads and other hard surfaces such as gravel and paved surfaces. GSP measurements were not taken on highly reflective surfaces such as center line stripes or lane markings on roads due to the increased noise seen in the laser returns over these surfaces. GSPs were collected within as many flightlines as possible; however, the distribution of GSPs depended on ground access constraints and monument locations and may not be equitably distributed throughout the study area (Figure 3).

Table 6: QSI ground survey equipment identification

Receiver Model	Antenna	OPUS Antenna ID	Use
Trimble R7 GNSS	Zephyr GNSS Geodetic Model 2 RoHS	TRM57971.00	Static, Rover
Trimble R8	Integrated Antenna	TRM_R8_GNSS	Rover

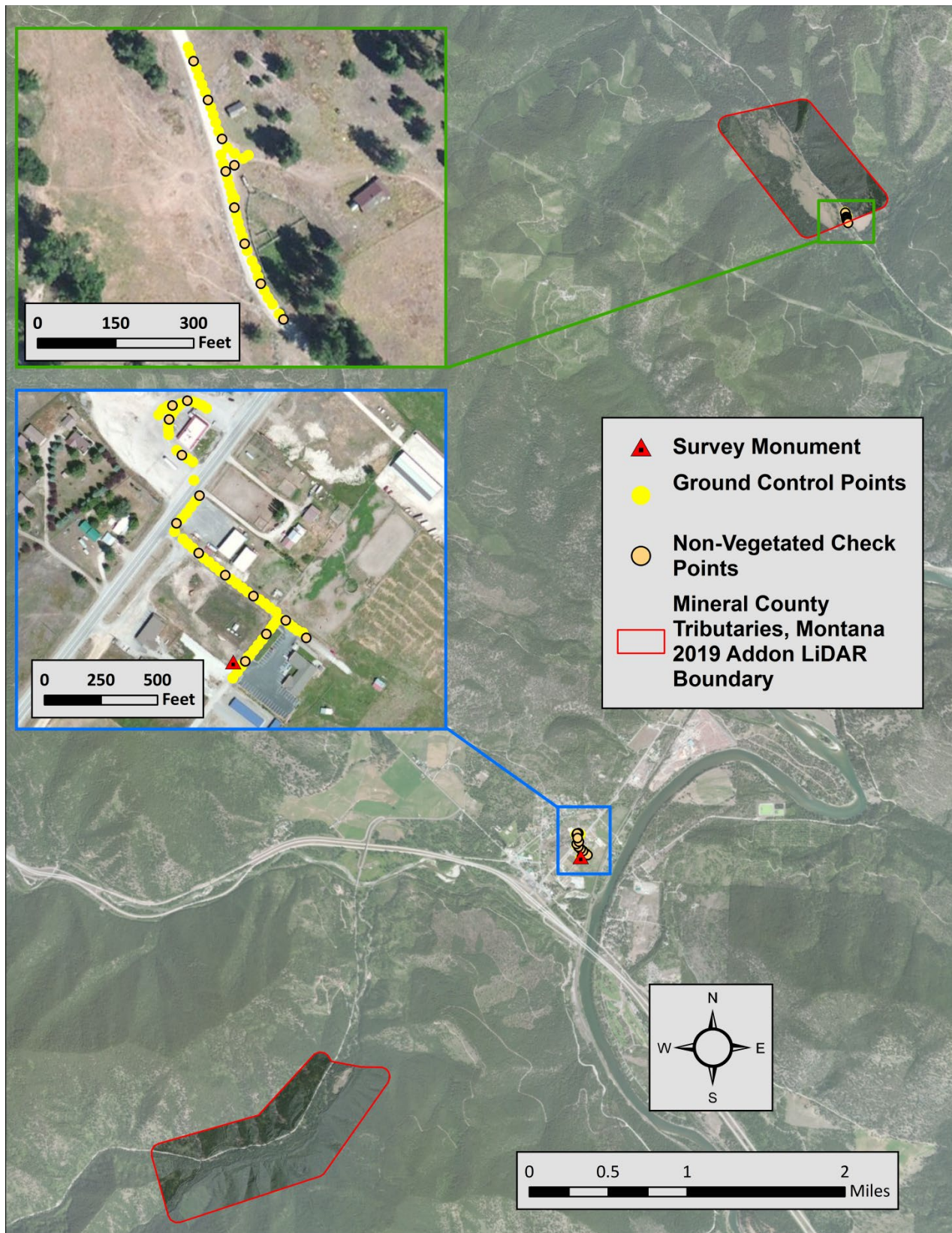
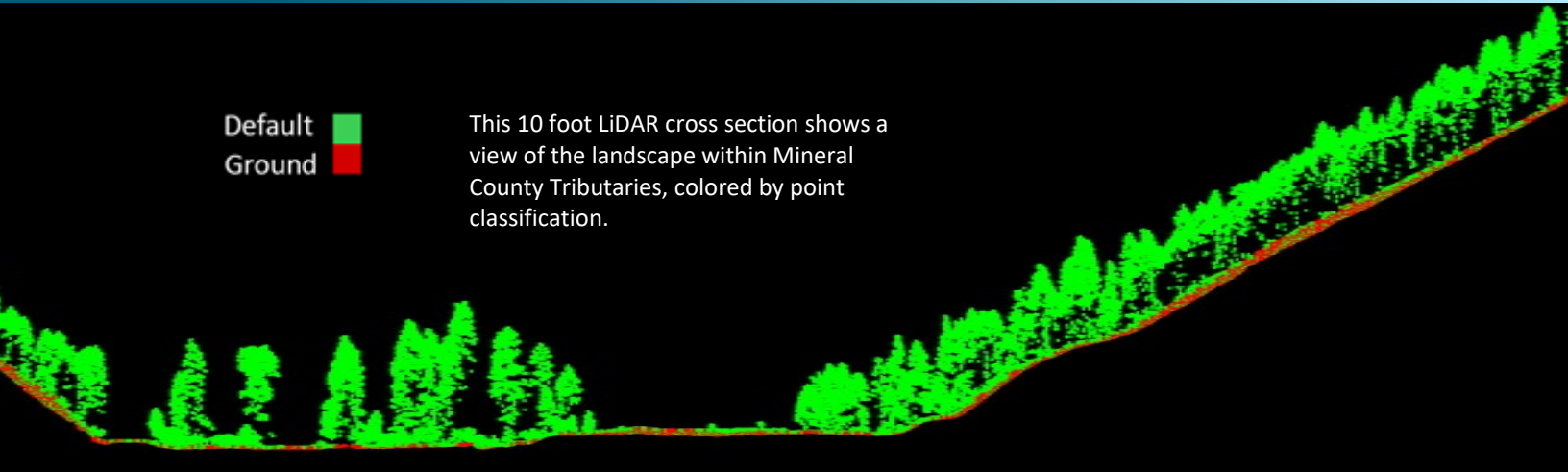


Figure 3: Ground survey location map

Default
Ground

This 10 foot LiDAR cross section shows a view of the landscape within Mineral County Tributaries, colored by point classification.



LiDAR Data

Upon completion of data acquisition, QSI processing staff initiated a suite of automated and manual techniques to process the data into the requested deliverables. Processing tasks included GPS control computations, smoothed best estimate trajectory (SBET) calculations, kinematic corrections, calculation of laser point position, sensor and data calibration for optimal relative and absolute accuracy, and LiDAR point classification (Table 7). Processing methodologies were tailored for the landscape. Brief descriptions of these tasks are shown in Table 8.

Table 7: ASPRS LAS classification standards applied to the Mineral County Tributaries dataset

Classification Number	Classification Name	Classification Description
1	Default/Unclassified	Laser returns that are not included in the ground class, composed of vegetation and anthropogenic features
2	Ground	Laser returns that are determined to be ground using automated and manual cleaning algorithms.
6	Buildings	Permanent structures with a minimum area 100 ft ² or larger, classified using automated routines.
7	Noise	Laser returns that are often associated with birds, scattering from reflective surfaces, or artificial points below the ground surface.
25	Water Column	Refracted Riegl sensor returns that are determined to be water using automated and manual cleaning algorithms. *Clark Fork Reprocessed AOI only
26	Bathymetric Bottom	Refracted Riegl sensor returns that fall within the water's edge breakline which characterize the submerged topography. *Clark Fork Reprocessed AOI only
27	Water Surface	Green laser returns that are determined to be water surface points using automated and manual cleaning algorithms. *Clark Fork Reprocessed AOI only

Table 8: LiDAR processing workflow

LiDAR Processing Step	Software Used
Resolve kinematic corrections for aircraft position data using kinematic aircraft GPS and static ground GPS data. Develop a smoothed best estimate of trajectory (SBET) file that blends post-processed aircraft position with sensor head position and attitude recorded throughout the survey.	Waypoint Inertial Explorer v.8.7
Calculate laser point position by associating SBET position to each laser point return time, scan angle, intensity, etc. Create raw laser point cloud data for the entire survey in *.las (ASPRS v. 1.2) format. Convert data to orthometric elevations by applying a geoid correction.	Leica Cloudpro v. 1.2.4
Import raw laser points into manageable blocks to perform manual relative accuracy calibration and filter erroneous points. Classify ground points for individual flight lines.	TerraScan v.19
Using ground classified points per each flight line, test the relative accuracy. Perform automated line-to-line calibrations for system attitude parameters (pitch, roll, heading), mirror flex (scale) and GPS/IMU drift. Calculate calibrations on ground classified points from paired flight lines and apply results to all points in a flight line. Use every flight line for relative accuracy calibration.	TerraMatch v.19
Apply refraction correction to all subsurface returns within the Clark Fork reprocessed AOI.	Las Monkey 2.4.2 (QSI proprietary software)
Classify resulting data to ground and other client designated ASPRS classifications (Table 7). Assess statistical absolute accuracy via direct comparisons of ground classified points to ground control survey data.	TerraScan v.19 TerraModeler v.19
Generate bare earth models as triangulated surfaces. Export all surface models as GeoTIFFs (*.Tif) at a 3.0 foot pixel resolution.	LAS Product Creator 3.3 (QSI proprietary)
Generate contour lines from classified contour keypoints. Export all contours as polyline shapefiles.	TerraScan v.19 TerraModeler v.19 ArcMap v. 10.3.1

Bathymetric Refraction

The water surface models used for refraction are generated using elevation information derived from the NIR channel to inform where the green water surface level is located, and then water surface points are classified for both the forward and reverse look directions of the green scanner. Points are filtered and edited to obtain the most accurate representation of the water surface and are used to create a water surface model for each flight line and look direction. Water surface classification and modeling is processed on each flight line to accommodate water level changes due to tide and temporal changes in water surface. Each look direction (forward and reverse) are modeled separately to correctly model short duration time dependent surface changes that change between the times that each look direction records a unique location. The water surface model created is raster based with an associated surface normal vector to obtain the most accurate angle of incidence during refraction. The refraction processing is done using the proprietary Quantum Spatial software Las Monkey.

LiDAR Derived Products

Because hydrographic laser scanners penetrate the water surface to map submerged topography, this affects how the data should be processed and presented in derived products from the LiDAR point cloud. The following discusses certain derived products that vary from the traditional (NIR) specification and delivery format.

Topobathymetric DEMs

Bathymetric bottom returns can be limited by depth, water clarity, and bottom surface reflectivity. Water clarity and turbidity affects the depth penetration capability of the green wavelength laser with returning laser energy diminishing by scattering throughout the water column. Additionally, the bottom surface must be reflective enough to return remaining laser energy back to the sensor at a detectable level. Although the predicted depth penetration range of the Riegl VQ-880-G sensor is 1.5 Secchi depths on brightly reflective surfaces, it is not unexpected to have no bathymetric bottom returns in turbid or non-reflective areas.

As a result, creating digital elevation models (DEMs) presents a challenge with respect to interpolation of areas with no returns. Traditional DEMs are “unclipped”, meaning areas lacking ground returns are interpolated from neighboring ground returns (or breaklines in the case of hydro-flattening), with the assumption that the interpolation is close to reality. In bathymetric modeling, these assumptions are prone to error because a lack of bathymetric returns can indicate a change in elevation that the laser can no longer map due to increased depths. The resulting void areas may suggest greater depths, rather than similar elevations from neighboring bathymetric bottom returns. Therefore, QSI created a water polygon with bathymetric coverage to delineate areas with successfully mapped bathymetry. This shapefile was used to control the extent of the delivered clipped topobathymetric model to avoid false triangulation (interpolation from TIN’ing) across areas in the water with no bathymetric returns.

Contours

Contour generation from LiDAR point data required a thinning operation in order to reduce contour sinuosity. The thinning operation reduced point density where topographic change is minimal (i.e., flat surfaces) while preserving resolution where topographic change was present. Model key points were selected from the ground model by interpolating between contour key points at even elevation increments. Generation of model key points eliminated redundant detail in terrain representation, particularly in areas of low relief, and provided for a more manageable dataset.

Ground point density rasters were developed to identify areas of low confidence within the contour lines. Areas greater than two acres with an average point density of less than .05 points/ft² are described as low confidence. No areas defined as low confidence exist within the Mineral County Tributaries dataset.

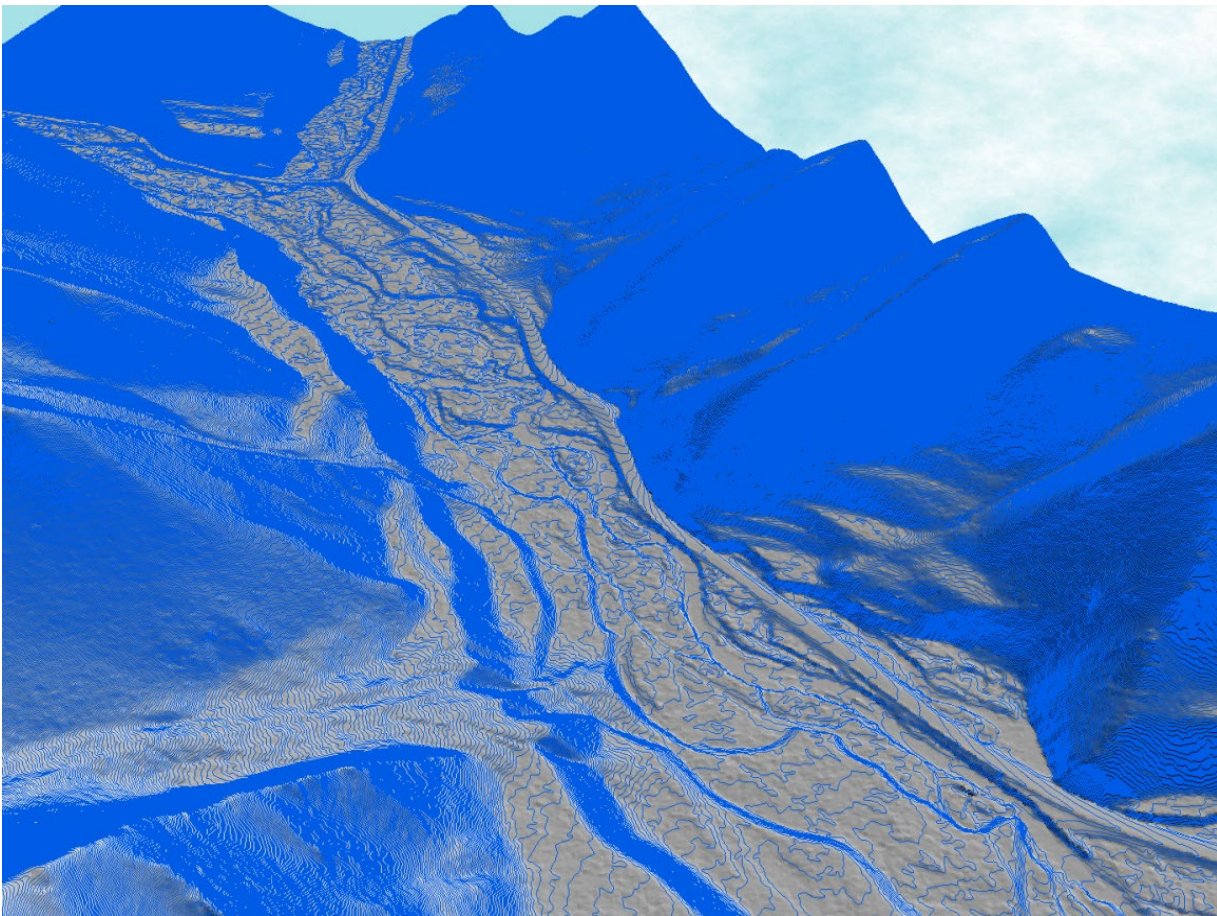
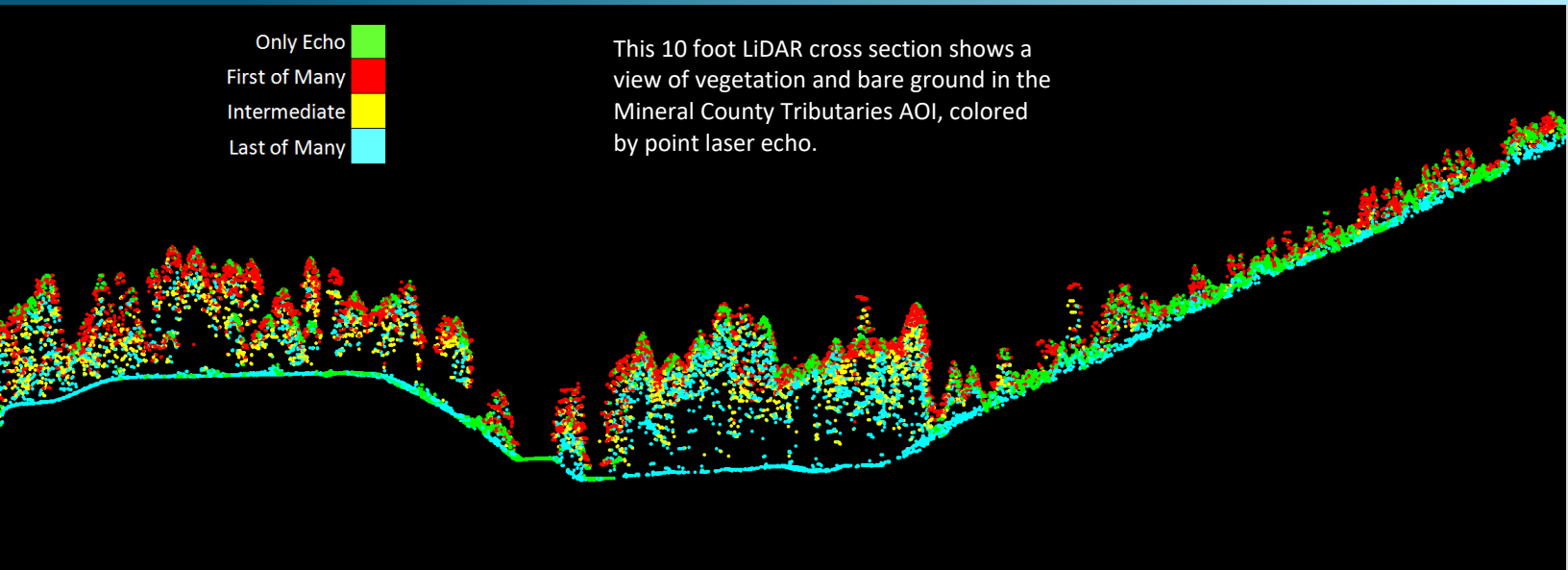


Figure 4: Contours draped over the Mineral County Tributaries bare earth elevation model

Only Echo ■
First of Many ■
Intermediate ■
Last of Many ■

This 10 foot LiDAR cross section shows a view of vegetation and bare ground in the Mineral County Tributaries AOI, colored by point laser echo.



LiDAR Density

The acquisition parameters were designed to acquire an average first-return density of 8 points/m² (0.74 points/ft²). First return density describes the density of pulses emitted from the laser that return at least one echo to the system. Multiple returns from a single pulse were not considered in first return density analysis. Some types of surfaces (e.g., breaks in terrain, water and steep slopes) may have returned fewer pulses than originally emitted by the laser. First returns typically reflect off the highest feature on the landscape within the footprint of the pulse. In forested or urban areas the highest feature could be a tree, building or power line, while in areas of unobstructed ground, the first return will be the only echo and represents the bare earth surface.

The density of ground-classified LiDAR returns was also analyzed for this project. Terrain character, land cover, and ground surface reflectivity all influenced the density of ground surface returns. In vegetated areas, fewer pulses may penetrate the canopy, resulting in lower ground density.

The average first-return density of LiDAR data for the Mineral County Tributaries 2019 LiDAR acquisition was 1.16/ft² (12.53 points/m²) while the average ground classified density was 0.25 points/ft² (2.66 points/m²). For reprocessed areas corresponding to the 2016 and 2017 LiDAR acquisitions, the average first-return density of LiDAR data was 1.69 points/ft² (18.23 points/m²) while the average ground classified density was 0.47 points/ft² (5.03 points/m²) (Table 9).

Additionally, for the reprocessed topobathymetric portion corresponding to the 2016 Clark Fork Acquisition, density values of only bathymetric returns were calculated for areas containing at least one bathymetric bottom return. Areas lacking bathymetric returns were not considered in calculating an average density value. Within the successfully mapped area, a bathymetric bottom return density of 0.51 points/ft² (5.51 points/m²) was achieved. The statistical and spatial distributions of first return densities and classified ground return densities per 100 m x 100 m cell are portrayed in Figure 5 through Figure 11.

Table 9: Average LiDAR point densities

Classification	Point Density 2019 Acquisition	Point Density 2016-2017 Acquisitions
First-Return	1.16 points/ft ² 12.53 points/m ²	1.69 points/ft ² 18.23 points/m ²
Ground Classified	0.25 points/ft ² 2.66 points/m ²	0.47 points/ft ² 5.03 points/m ²

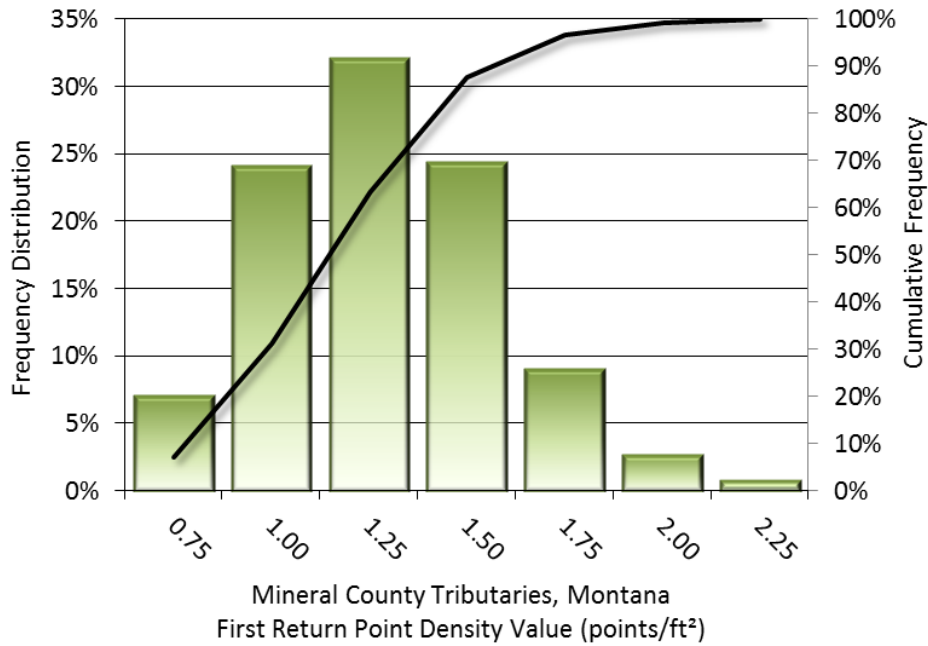


Figure 5: Frequency distribution of first return point density values of 2019 acquisition per 100 x 100 m cell

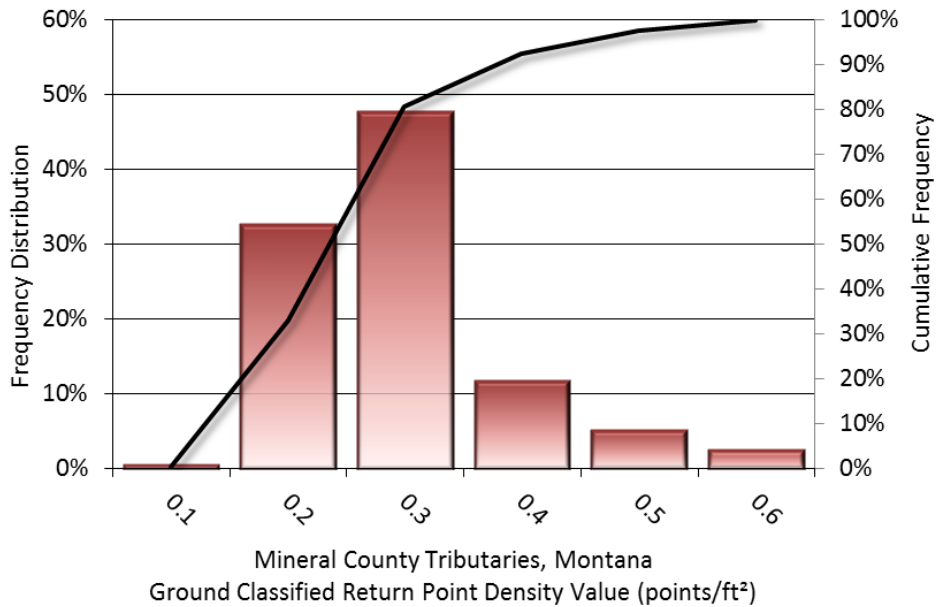


Figure 6: Frequency distribution of ground-classified return point density values of 2019 acquisition per 100 x 100 m cell

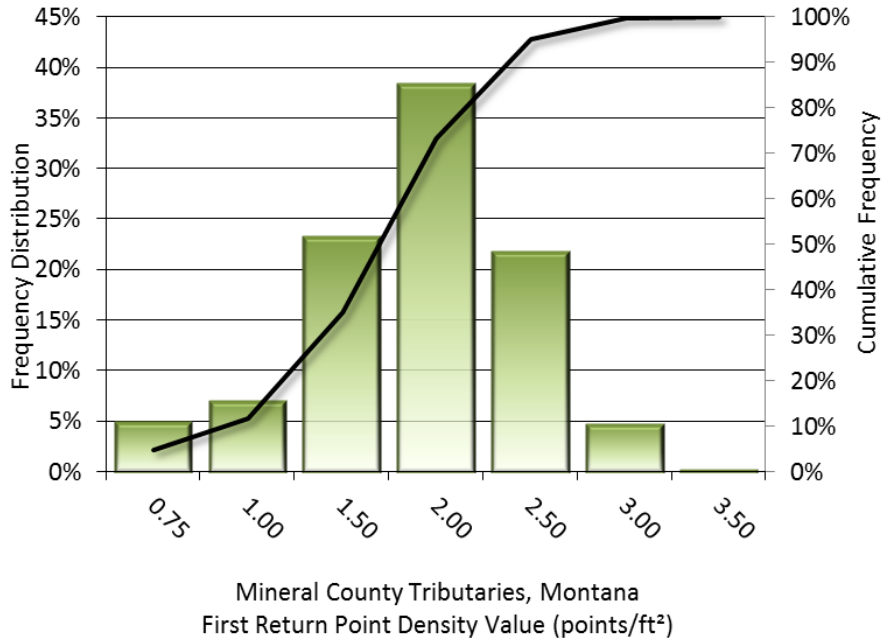


Figure 7: Frequency distribution of first return point density values of 2016-2017 acquisitions per 100 x 100 m cell

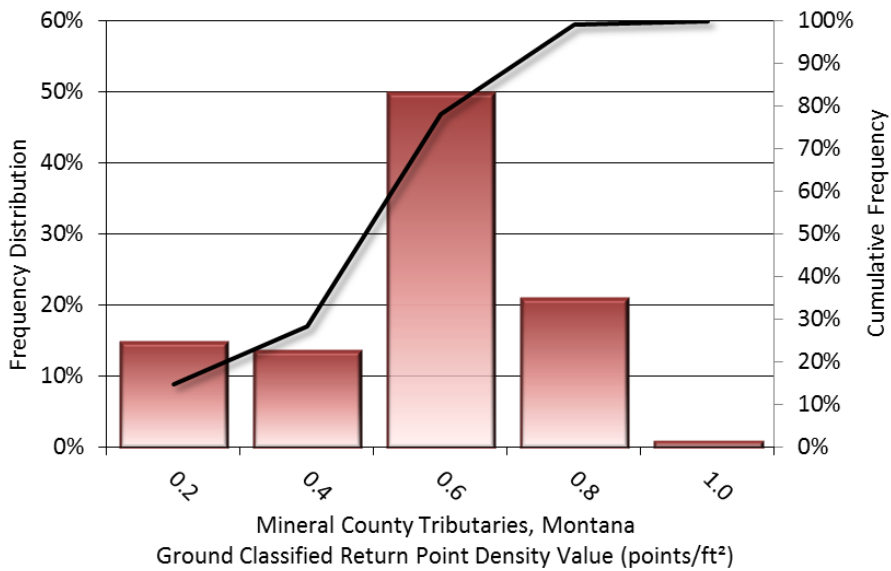


Figure 8: Frequency distribution of ground-classified return point density values of 2016-2017 acquisitions per 100 x 100 m cell

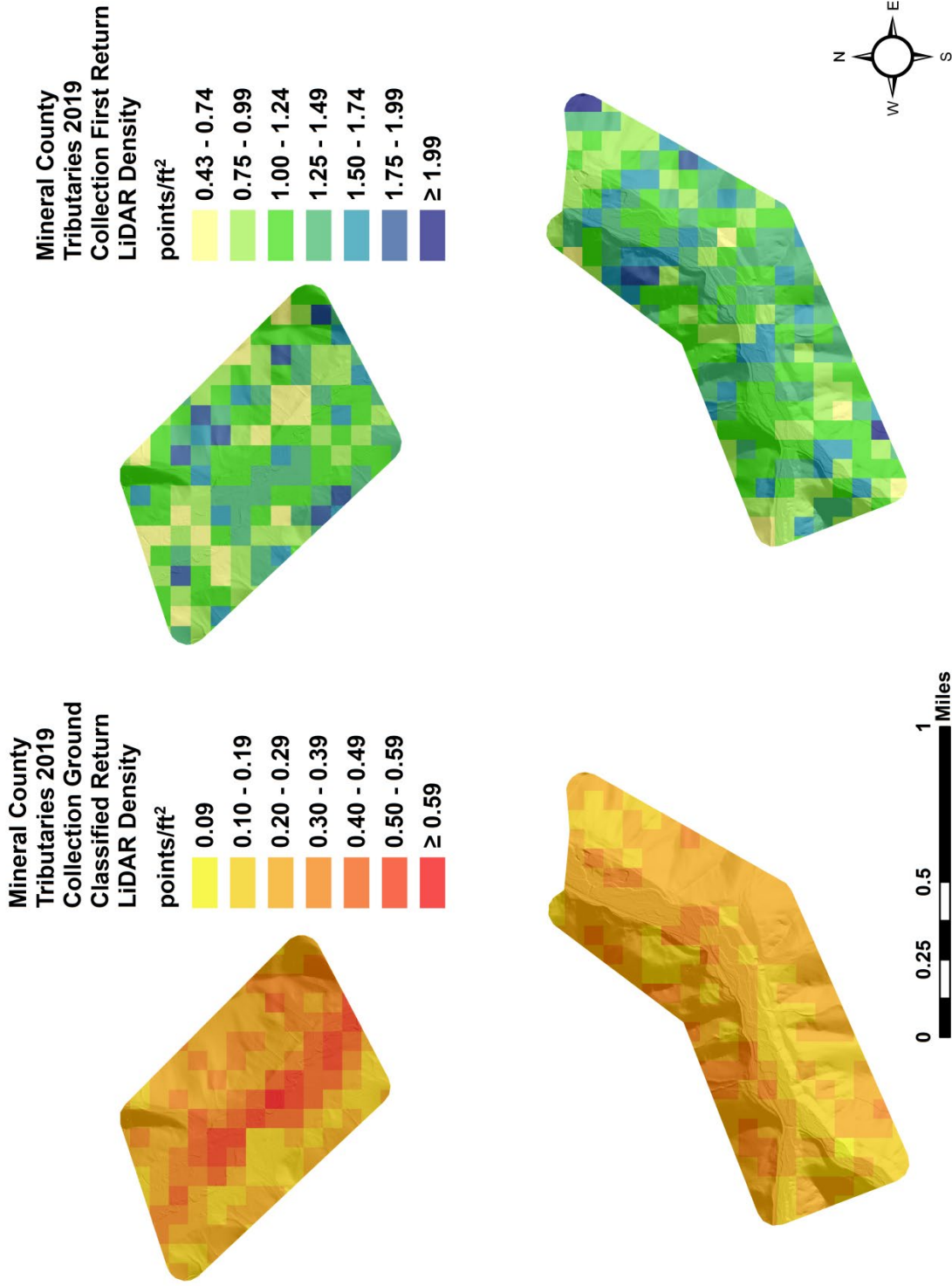


Figure 9 : First return and ground-classified point density map for the Mineral County Tributaries 2019 LiDAR Acquisition (100 m x 100 m cells)

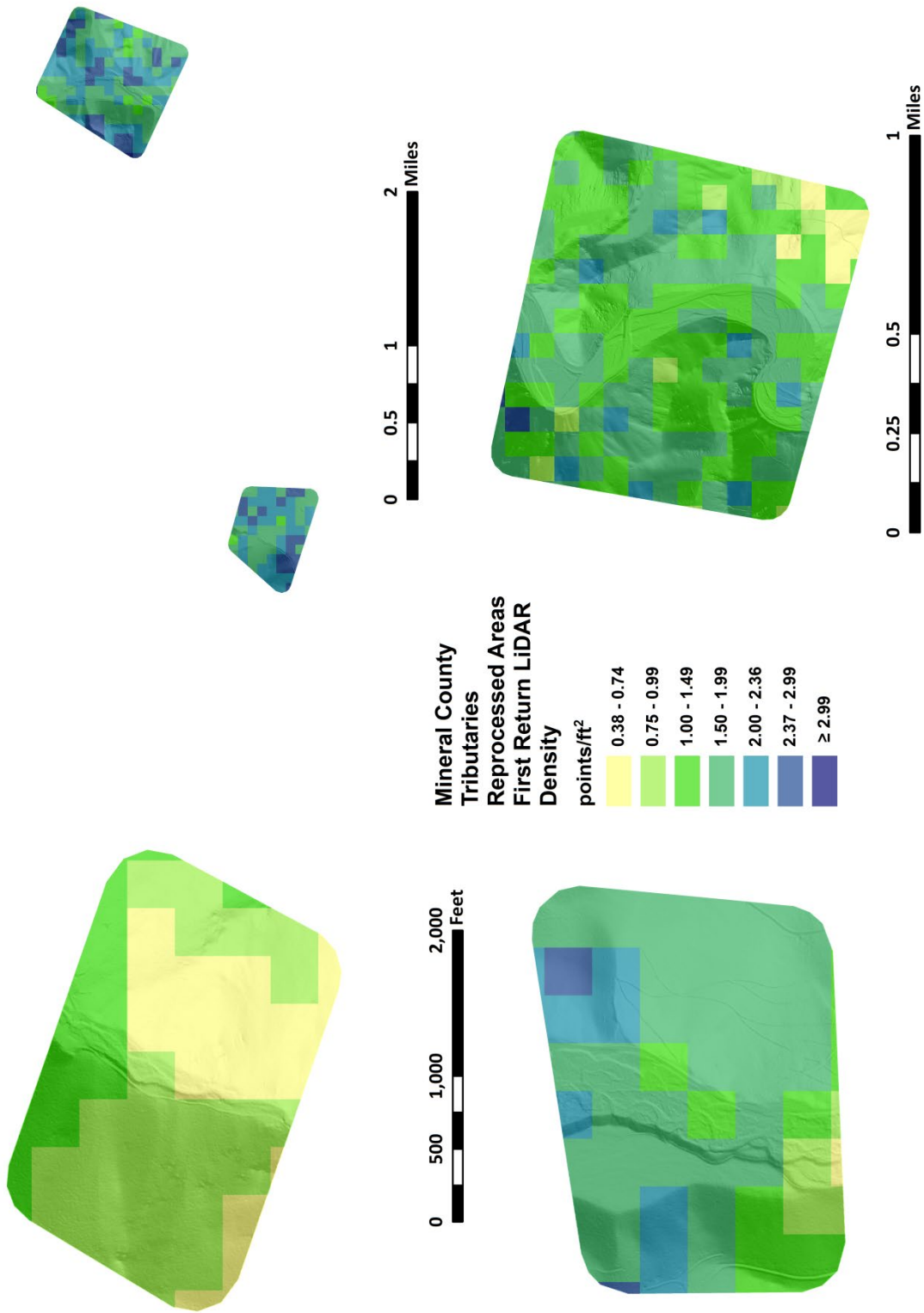


Figure 10: First return density map for the Mineral County Tributaries site 2016-2017 LiDAR acquisitions (100 m x 100 m cells)

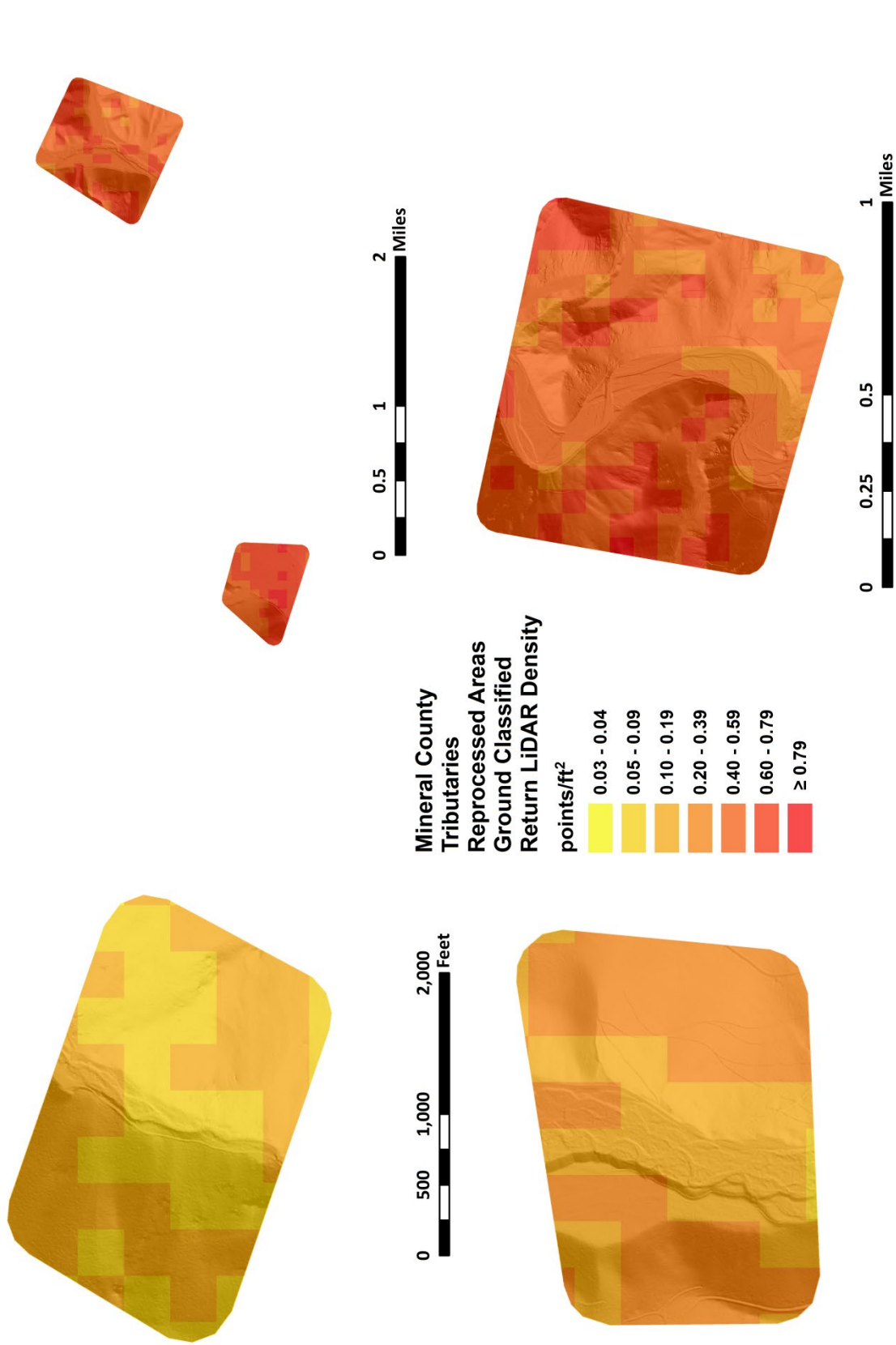


Figure 11: Ground classified return density map for the Mineral County Tributaries site 2016-2017 LiDAR acquisitions (100 m x 100 m cells)

LiDAR Accuracy Assessments

The accuracy of the LiDAR data collection can be described in terms of absolute accuracy (the consistency of the data with external data sources) and relative accuracy (the consistency of the dataset with itself). See Appendix A for further information on sources of error and operational measures used to improve relative accuracy.

LiDAR Non-Vegetated Vertical Accuracy

Absolute accuracy was assessed using Non-Vegetated Vertical Accuracy (NVA) reporting designed to meet guidelines presented in the FGDC National Standard for Spatial Data Accuracy³. NVA compares known ground check point data that were withheld from the calibration and post-processing of the LiDAR point cloud to the triangulated surface generated by the unclassified LiDAR point cloud as well as the derived gridded bare earth DEM. NVA is a measure of the accuracy of LiDAR point data in open areas where the LiDAR system has a high probability of measuring the ground surface and is evaluated at the 95% confidence interval ($1.96 * RMSE$), as shown in Table 10.

The mean and standard deviation (sigma σ) of divergence of the ground surface model from quality assurance point coordinates are also considered during accuracy assessment. These statistics assume the error for x, y and z is normally distributed, and therefore the skew and kurtosis of distributions are also considered when evaluating error statistics. For the Mineral County Tributaries 2019 survey, 22 ground check points were withheld from the calibration and post processing of the LiDAR point cloud, with resulting non-vegetated vertical accuracy of 0.104 feet (0.032 meters) as compared to unclassified LAS, and 0.100 feet (0.031 meters) as compared to the bare earth DEM, with 95% confidence (Figure 12, Figure 13).

QSI also assessed absolute accuracy using 88 ground control points. Although these points were used in the calibration and post-processing of the LiDAR point cloud, they still provide a good indication of the overall accuracy of the LiDAR dataset, and therefore have been provided in Table 10 and Figure 14. Please see the LiDAR accuracy assessment section within the St. Regis and Clark Fork technical data reports for accuracy statistics pertaining to the Mineral County Tributaries reprocessed areas of interest.

³ Federal Geographic Data Committee, ASPRS POSITIONAL ACCURACY STANDARDS FOR DIGITAL GEOSPATIAL DATA EDITION 1, Version 1.0, NOVEMBER 2014. <http://www.asprs.org/PAD-Division/ASPRS-POSITIONAL-ACCURACY-STANDARDS-FOR-DIGITAL-GEOSPATIAL-DATA.html>.

Table 10: Absolute accuracy results

Absolute Vertical Accuracy			
	NVA, as compared to unclassified LAS	NVA, as compared to bare earth DEM	Ground Control Points
Sample	22 points	22 points	88 points
95% Confidence (1.96*RMSE)	0.104 ft 0.032 m	0.100 ft 0.031 m	0.076 ft 0.023 m
Average	0.022 ft 0.007 m	0.029 ft 0.009 m	0.000 ft 0.000 m
Median	0.015 ft 0.005 m	0.033 ft 0.010 m	0.000 ft 0.000 m
RMSE	0.053 ft 0.016 m	0.051 ft 0.016 m	0.039 ft 0.012 m
Standard Deviation (1σ)	0.049 ft 0.015 m	0.044 ft 0.013 m	0.039 ft 0.012 m

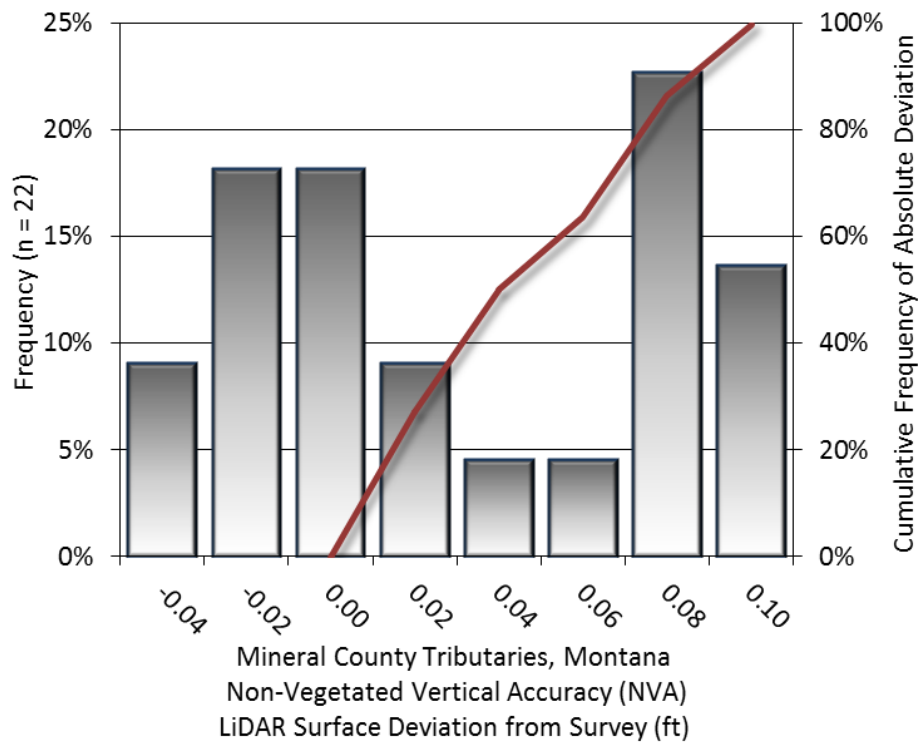


Figure 12: Frequency histogram for LiDAR unclassified LAS deviation from ground check point values (NVA)

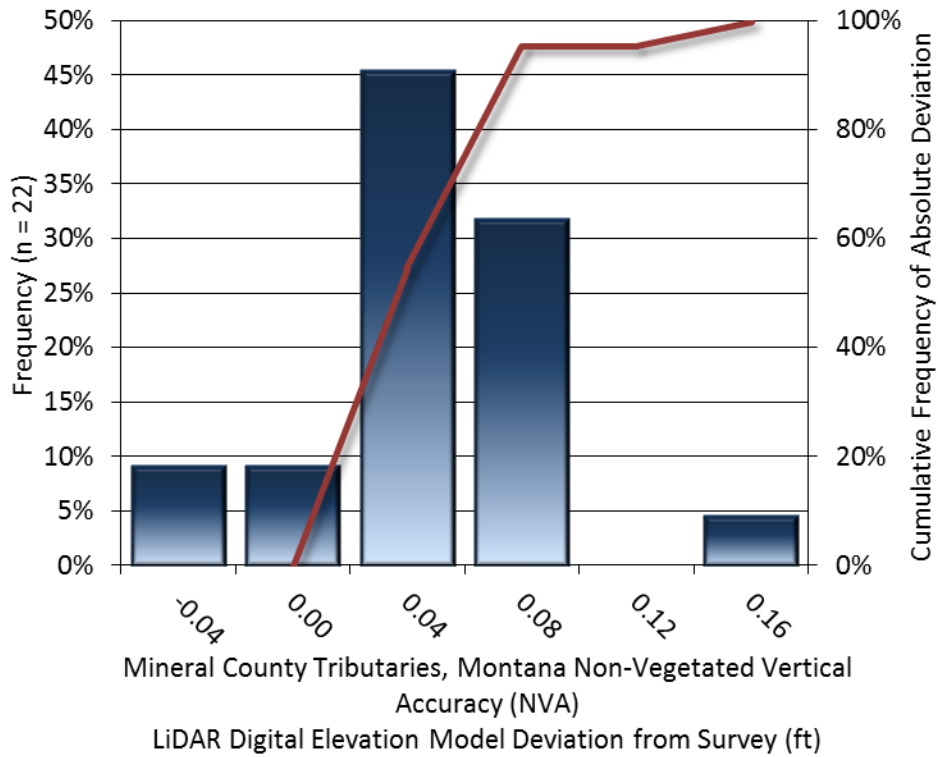


Figure 13: Frequency histogram for LiDAR bare earth DEM surface deviation from ground check point values (NVA)

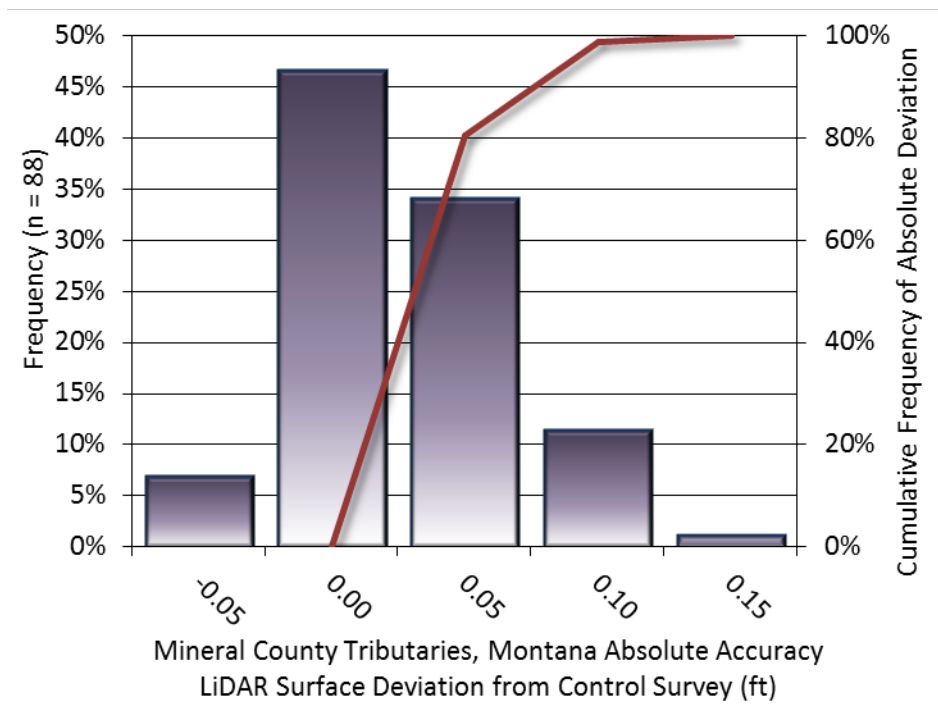


Figure 14: Frequency histogram for LiDAR surface deviation from ground control point values

LiDAR Relative Vertical Accuracy

Relative vertical accuracy refers to the internal consistency of the data set as a whole: the ability to place an object in the same location given multiple flight lines, GPS conditions, and aircraft attitudes. When the LiDAR system is well calibrated, the swath-to-swath vertical divergence is low (<0.10 meters). The relative vertical accuracy was computed by comparing the ground surface model of each individual flight line with its neighbors in overlapping regions. The average (mean) line to line relative vertical accuracy for the Mineral County Tributaries 2019 LiDAR acquisition was 0.182 feet (0.056 meters) (Table 11, Figure 15).

Table 11: Relative accuracy results

Relative Accuracy	
Sample	11 surfaces
Average	0.182 ft 0.056 m
Median	0.176 ft 0.054 m
RMSE	0.184 ft 0.056 m
Standard Deviation (1σ)	0.101 ft 0.031 m
1.96 σ	0.101 ft 0.031 m

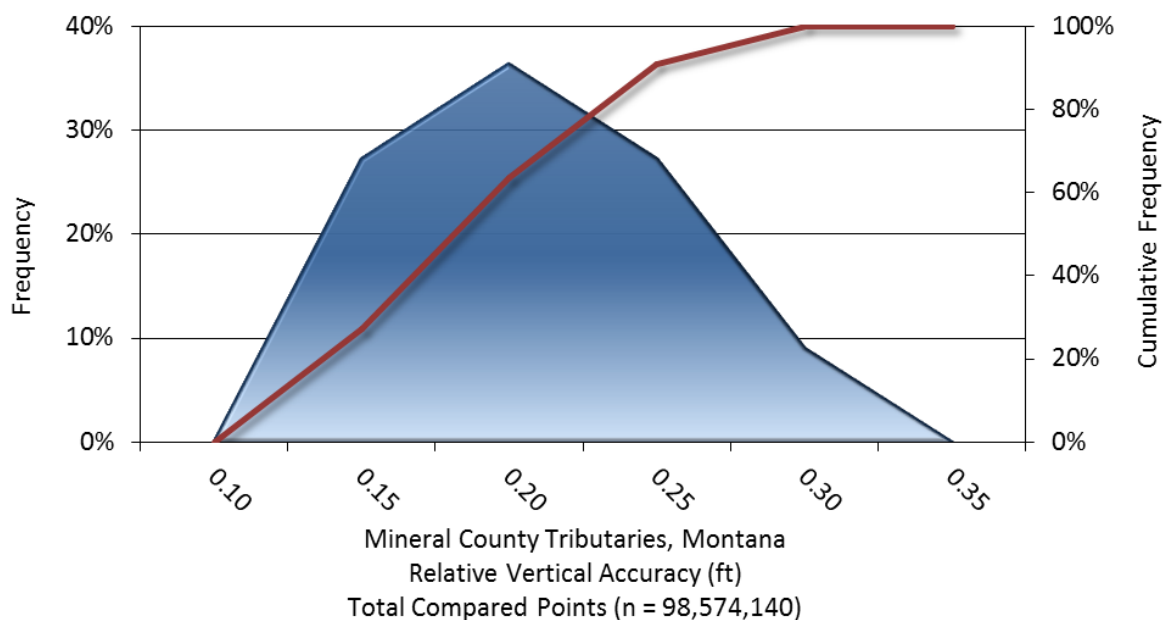


Figure 15: Frequency plot for relative vertical accuracy between flight lines

LiDAR Horizontal Accuracy

LiDAR horizontal accuracy is a function of Global Navigation Satellite System (GNSS) derived positional error, flying altitude, and INS-derived attitude error. The obtained $RMSE_r$ value is multiplied by a conversion factor of 1.7308 to yield the horizontal component (ACC_r) of the National Standards for Spatial Data Accuracy (NSSDA) reporting standard where a theoretical point will fall within the obtained radius 95 percent of the time. Using a flying altitude of 1,900 meters, an IMU error of 0.0068 decimal degrees, and a GNSS positional error of 0.032 meters, the horizontal accuracy for the 2019 LiDAR collection is 0.40 meters (1.31 feet) at the 95% confidence level. The 2016 Clark Fork and 2017 St. Regis project sites have horizontal accuracy values of 0.25 meters (0.83 feet) and 0.06 meters (0.18 feet) respectively (Table 12). Data from the Mineral County Tributaries dataset have been tested to meet horizontal requirements at the 95% confidence level, using NSSDA reporting methods.

Table 12: Horizontal Accuracy

Horizontal Accuracy			
Site	2016 Clark Fork Acquisition	2017 St. Regis Acquisition	2019 Mineral County Tributaries Acquisition
RMSE _r	0.48 ft	0.11 ft	0.76 ft
	0.15 m	0.03 m	0.23 m
ACC _r	0.83 ft	0.18 ft	1.31 ft
	0.25 m	0.06 m	0.40 m

CERTIFICATIONS

Quantum Spatial, Inc. provided LiDAR services for the Mineral County Tributaries project as described in this report.

I, Ashley Daigle, have reviewed the attached report for completeness and hereby state that it is a complete and accurate report of this project.

Ashley Daigle

Ashley Daigle
Project Manager
Quantum Spatial, Inc.

Jul 10, 2019

I, Steven J. Hyde, PLS, being duly registered as a Professional Land Surveyor in and by the state of Montana, hereby certify that the methodologies, static GNSS occupations used during airborne flights, and ground survey point collection were performed using commonly accepted Standard Practices. Field work conducted for this report was conducted on May 5, 2019.

Accuracy statistics shown in the Accuracy Section of this Report have been reviewed by me and found to meet the "National Standard for Spatial Data Accuracy".

Steven J. Hyde



Steven J. Hyde, PLS
Quantum Spatial, Inc.
Corvallis, OR 97330

July 09, 2019

SELECTED IMAGE

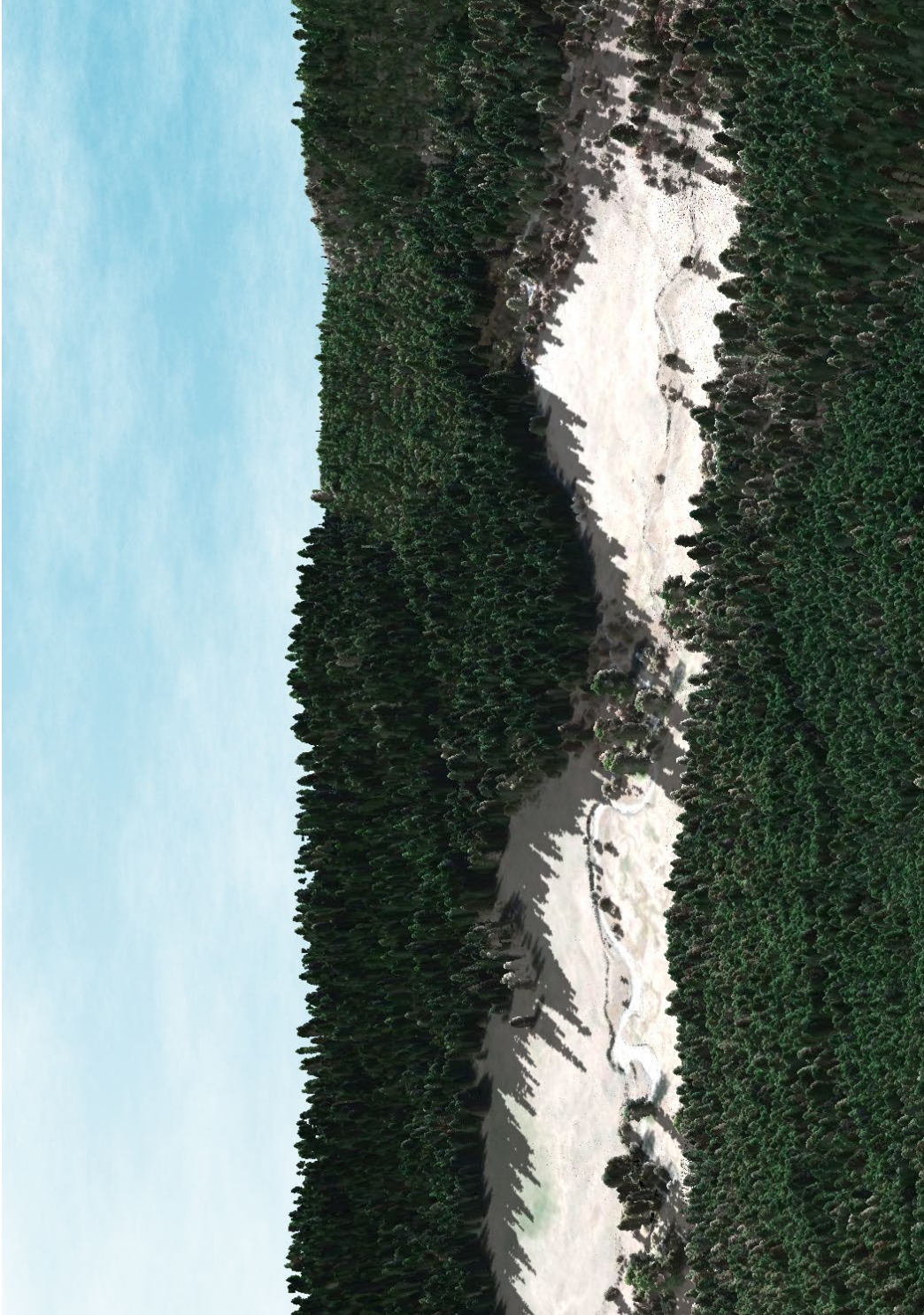


Figure 16: A view looking southwest at Tamarack Creek within the northernmost AOI of the 2019 LiDAR acquisition. The image was created from the LiDAR bare earth model colored by elevation and overlaid with Virtual Earth Satellite imagery and the above ground point cloud.

1-sigma (σ) Absolute Deviation: Value for which the data are within one standard deviation (approximately 68th percentile) of a normally distributed data set.

1.96 * RMSE Absolute Deviation: Value for which the data are within two standard deviations (approximately 95th percentile) of a normally distributed data set, based on the FGDC standards for Non-vegetated Vertical Accuracy (NVA) reporting.

Accuracy: The statistical comparison between known (surveyed) points and laser points. Typically measured as the standard deviation (σ) and root mean square error (RMSE).

Absolute Accuracy: The vertical accuracy of LiDAR data is described as the mean and standard deviation (σ) of divergence of LiDAR point coordinates from ground survey point coordinates. To provide a sense of the model predictive power of the dataset, the root mean square error (RMSE) for vertical accuracy is also provided. These statistics assume the error distributions for x, y and z are normally distributed, and thus we also consider the skew and kurtosis of distributions when evaluating error statistics.

Relative Accuracy: Relative accuracy refers to the internal consistency of the data set; i.e., the ability to place a laser point in the same location over multiple flight lines, GPS conditions and aircraft attitudes. Affected by system attitude offsets, scale and GPS/IMU drift, internal consistency is measured as the divergence between points from different flight lines within an overlapping area. Divergence is most apparent when flight lines are opposing. When the LiDAR system is well calibrated, the line-to-line divergence is low (<10 cm).

Root Mean Square Error (RMSE): A statistic used to approximate the difference between real-world points and the LiDAR points. It is calculated by squaring all the values, then taking the average of the squares and taking the square root of the average.

Data Density: A common measure of LiDAR resolution, measured as points per square meter.

Digital Elevation Model (DEM): File or database made from surveyed points, containing elevation points over a contiguous area. Digital terrain models (DTM) and digital surface models (DSM) are types of DEMs. DTMs consist solely of the bare earth surface (ground points), while DSMs include information about all surfaces, including vegetation and man-made structures.

Intensity Values: The peak power ratio of the laser return to the emitted laser, calculated as a function of surface reflectivity.

Nadir: A single point or locus of points on the surface of the earth directly below a sensor as it progresses along its flight line.

Overlap: The area shared between flight lines, typically measured in percent. 100% overlap is essential to ensure complete coverage and reduce laser shadows.

Pulse Rate (PR): The rate at which laser pulses are emitted from the sensor; typically measured in thousands of pulses per second (kHz).

Pulse Returns: For every laser pulse emitted, the number of wave forms (i.e., echoes) reflected back to the sensor. Portions of the wave form that return first are the highest element in multi-tiered surfaces such as vegetation. Portions of the wave form that return last are the lowest element in multi-tiered surfaces.

Real-Time Kinematic (RTK) Survey: A type of surveying conducted with a GPS base station deployed over a known monument with a radio connection to a GPS rover. Both the base station and rover receive differential GPS data and the baseline correction is solved between the two. This type of ground survey is accurate to 1.5 cm or less.

Post-Processed Kinematic (PPK) Survey: GPS surveying is conducted with a GPS rover collecting concurrently with a GPS base station set up over a known monument. Differential corrections and precisions for the GNSS baselines are computed and applied after the fact during processing. This type of ground survey is accurate to 1.5 cm or less.

Scan Angle: The angle from nadir to the edge of the scan, measured in degrees. Laser point accuracy typically decreases as scan angles increase.

Native LiDAR Density: The number of pulses emitted by the LiDAR system, commonly expressed as pulses per square meter.

APPENDIX A - ACCURACY CONTROLS

Relative Accuracy Calibration Methodology:

Manual System Calibration: Calibration procedures for each mission require solving geometric relationships that relate measured swath-to-swath deviations to misalignments of system attitude parameters. Corrected scale, pitch, roll and heading offsets were calculated and applied to resolve misalignments. The raw divergence between lines was computed after the manual calibration was completed and reported for each survey area.

Automated Attitude Calibration: All data were tested and calibrated using TerraMatch automated sampling routines. Ground points were classified for each individual flight line and used for line-to-line testing. System misalignment offsets (pitch, roll and heading) and scale were solved for each individual mission and applied to respective mission datasets. The data from each mission were then blended when imported together to form the entire area of interest.

Automated Z Calibration: Ground points per line were used to calculate the vertical divergence between lines caused by vertical GPS drift. Automated Z calibration was the final step employed for relative accuracy calibration.

LiDAR accuracy error sources and solutions:

Type of Error	Source	Post Processing Solution
GPS (Static/Kinematic)	Long Base Lines	None
	Poor Satellite Constellation	None
	Poor Antenna Visibility	Reduce Visibility Mask
Relative Accuracy	Poor System Calibration	Recalibrate IMU and sensor offsets/settings
	Inaccurate System	None
Laser Noise	Poor Laser Timing	None
	Poor Laser Reception	None
	Poor Laser Power	None
	Irregular Laser Shape	None

Operational measures taken to improve relative accuracy:

Low Flight Altitude: Terrain following was employed to maintain a constant above ground level (AGL). Laser horizontal errors are a function of flight altitude above ground (about 1/3000th AGL flight altitude).

Focus Laser Power at narrow beam footprint: A laser return must be received by the system above a power threshold to accurately record a measurement. The strength of the laser return (i.e., intensity) is a function of laser emission power, laser footprint, flight altitude and the reflectivity of the target. While surface reflectivity cannot be controlled, laser power can be increased and low flight altitudes can be maintained.

Reduced Scan Angle: Edge-of-scan data can become inaccurate. The scan angle was reduced to a maximum of $\pm 15^\circ$ from nadir, creating a narrow swath width and greatly reducing laser shadows from trees and buildings.

Quality GPS: Flights took place during optimal GPS conditions (e.g., 6 or more satellites and PDOP [Position Dilution of Precision] less than 3.0). Before each flight, the PDOP was determined for the survey day. During all flight times, a dual frequency DGPS base station recording at 1 second epochs was utilized and a maximum baseline length between the aircraft and the control points was less than 13 nm at all times.

Ground Survey: Ground survey point accuracy (<1.5 cm RMSE) occurs during optimal PDOP ranges and targets a minimal baseline distance of 4 miles between GPS rover and base. Robust statistics are, in part, a function of sample size (n) and distribution. Ground survey points are distributed to the extent possible throughout multiple flight lines and across the survey area.

50% Side-Lap (100% Overlap): Overlapping areas are optimized for relative accuracy testing. Laser shadowing is minimized to help increase target acquisition from multiple scan angles. Ideally, with a 50% side-lap, the nadir portion of one flight line coincides with the swath edge portion of overlapping flight lines. A minimum of 50% side-lap with terrain-followed acquisition prevents data gaps.

Opposing Flight Lines: All overlapping flight lines have opposing directions. Pitch, roll and heading errors are amplified by a factor of two relative to the adjacent flight line(s), making misalignments easier to detect and resolve.